arXiv:2506.02849v1 [cs.RO] 3 Jun 2025

Learned Controllers for Agile Quadrotors in Pursuit-Evasion Games

Alejandro Sánchez Roncero, Olov Andersson and Petter Ögren

***Abstract*— The increasing proliferation of small UAVs in civilian and military airspace has raised critical safety and security concerns, especially when unauthorized or malicious drones enter restricted zones. In this work, we present a reinforcement learning (RL) framework for agile 1v1 quadrotor pursuit–evasion. We train neural network policies to command body rates and collective thrust, enabling high-speed pursuit and evasive maneuvers that fully exploit the quadrotor's nonlinear dynamics. To mitigate nonstationarity and catastrophic forgetting during adversarial co-training, we introduce an Asynchronous Multi-Stage Population-Based (AMSPB) algorithm where, at each stage, either the pursuer or evader learns against a sampled opponent drawn from a growing population of past and current policies. This continual learning setup ensures monotonic performance improvement and retention of earlier strategies. Our results show that (i) rate-based policies achieve significantly higher capture rates and peak speeds than velocity-level baselines, and (ii) AMSPB yields stable, monotonic gains against a suite of benchmark opponents.**

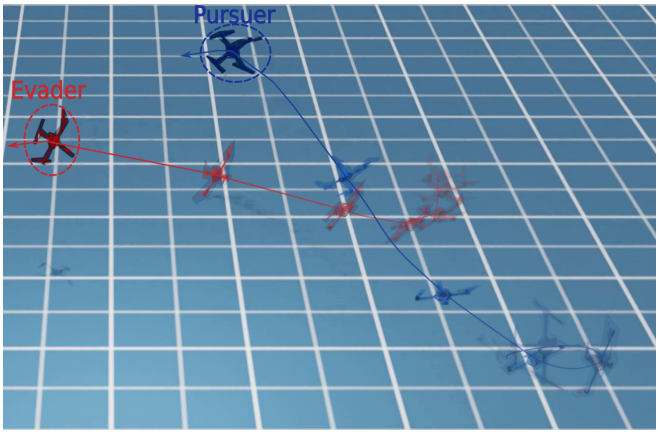

Fig. 1. 1v1 Pursuit-Evasion scenario using our learned AMSPB body-rate policies.

I. INTRODUCTION

In recent time we have seen a rapid proliferation of unmanned aerial vehicles (UAVs) in both civilian and military domains. In particular, unauthorized or malicious drones entering restricted zones pose significant safety and security risks, ranging from privacy violations and sabotage preparations to hostile attacks and mid-air collisions with manned aircraft [1]. Intercepting a moving intruder requires highly agile pursuit strategies to guarantee safe capture or neutralization [2], [3]. Traditional interception methods often assume a slow, waypoint-following evader or rely on overly simple vehicle kinematics, which in both cases fail to provide adequate responses when adversarial UAVs perform sudden evasive maneuvers or exploit their full dynamic capabilities. In a pursuit–evasion (PE) scenario, by contrast, the evader actively seeks to avoid capture, executing unpredictable maneuvers that can defeat simplistic interception strategies. Consequently, a future airspace security system that depends on pursuer UAVs, needs to be prepared for aggressive evader strategies.

Reinforcement learning (RL) offers a data-driven framework to jointly optimize perception, planning, and control in complex, nonstationary settings [4]. In drone racing, RL-based agents have demonstrated lap times that surpass those of expert human pilots by exploiting the full nonlinear quadrotor dynamics [5], [6], [4]. However, these racing problems assume either static waypoints (gates) or slowly moving targets to be reached and do not address the adversarial nature of an intelligent evader. When RL has been applied to PE games, prior works often simplify dynamics to 2D models [7], [8] or do not consider multiple opponent pursuer/evader strategies at the same time [9].

The main contributions of this work are:

- **Agile RL Controllers for both Pursuers and Evaders.** We provide RL policies controlling body rates and normalized thrust, and show that they outperform existing optimal control methods and RL policies outputting desired linear velocity.
- **Asynchronous Multi-Stage Population-Based (AMSPB) Training.** We propose a continual learning algorithm that alternates training between pursuer and evader agents, each time sampling from a growing population of opponent policies.

To the best of our knowledge, this has not been done for UAV pursuit-evasion problems using full 6 degrees of freedom models before.

The co-evolutionary setup of the AMSPB enables new tactics to be incorporated while older strategies are retained, reducing the risk of catastrophic forgetting and improving long-term robustness against new intruders' policies.

The long term goal of our research is to lay the groundwork for defender–intruder engagement strategies that can reliably secure urban airspace against unauthorized or malicious UAVs.

The remainder of this paper is organized as follows. Sec-

This work was partially supported by the Wallenberg AI, Autonomous Systems and Software Program (WASP) funded by the Knut and Alice Wallenberg Foundation. The authors are with the Robotics, Perception and Learning Lab., School of Electrical Engineering and Computer Science, Royal Institute of Technology (KTH), SE-100 44 Stockholm, Sweden alesr@kth.se Digital Object Identifier (DOI): see top of this page.

tion II reviews related work in RL for PE games. Section III introduces quadrotor dynamics. Our AMSPB methodology is detailed in Section IV, while Section V presents experimental results and ablation studies. Finally, Section VI provides the conclusions.

II. RELATED WORK

Classical interception and pursuit–evasion strategies often rely on model predictive control (MPC) or game-theoretic formulations that assume perfect state information and decouple planning from low-level control. For example, [10] proposes a variable time-step MPC that replans aggressive quadrotor trajectories to intercept dynamic targets in cluttered environments, while [3] designs a layered pipeline combining multi-sensor fusion, trajectory prediction, and MPC for safe mid-air interception. Although these model-based approaches achieve real-time performance, they typically assume a non-reactive intruder following some given path. They are therefore not designed nor tested against adversaries aggressively maneuvering to avoid interception.

Recently, reinforcement learning (RL) methods have been applied to both cooperative and adversarial UAV pursuit tasks to overcome the limitations of hand-designed controllers. In [2] Multi-Agent RL (MARL) was used for cooperative encirclement of unauthorized UAVs in urban airspace while [11] does multi-target pursuit by heterogeneous UAV swarms. Both methods demonstrate effective coordination but rely on simplified kinematic models and assume perfect global observations. Single-agent and paired-agent RL works, including [8], [9], [12], explore pursuit or evasion policies under partial observability, but typically output velocity-level commands and do not exploit the full nonlinear dynamics of quadrotors or directly reduce the complexity of the drone dynamics. In [4] a RL-comparison of body-rate versus velocity controllers in high-speed racing tasks showed that body-rate policies achieve significantly higher agility, suggesting that pursuit–evasion could likewise benefit from body-rate-level control.

The work that is closest to our paper is [9]. They propose an Asynchronous Multi-Stage DRL (AMS-DRL) algorithm that alternates training between pursuer and evader and converges to a Nash equilibrium. However, one drawback of their approach, as shown in Section V, is that the policies can overfit to an adversary, forgetting how to act against older adversaries and therefore being less useful against an unknown opponent. Moreover, they use velocity-based policies and simplify the dynamics of the drones, which limits agility and realism. Inspired by [9], we propose an Asynchronous Multi-Stage Population-Based (AMSPB) algorithm that continually samples from a growing set of past and current opponent policies to support monotonic improvement and mitigate forgetting. Finally, our policies control the body rates of the quadrotors, and we show in Section V that this leads to improved performance.

III. BACKGROUND

A. Quadrotor Dynamics

Each quadrotor is modeled as a rigid body of mass m and inertia tensor I. Let $p, v \in \mathbb{R}^3$ denote its position and velocity in the world frame, $R \in SO(3)$ the rotation matrix from body to world, and $\omega \in \mathbb{R}^3$ its body-frame angular velocity. Its continuous-time dynamics are the following [13]:

$$\dot{p} = v, \tag{1}$$

$$m\dot{v} = mg + R\sum_{i=1}^{4}\begin{bmatrix}0\\0\\T_i\end{bmatrix} + F_{\text{drag}} + F_{\text{downwash}}, \tag{2}$$

$$\dot{R} = R\,\widehat{\omega}, \tag{3}$$

$$I\,\dot{\omega} = -\,\omega \times (I\,\omega) + \sum_{i=1}^{4}\left(r_i \times \begin{bmatrix}0\\0\\T_i\end{bmatrix}\right) + \sum_{i=1}^{4}\tau_i u_i, \tag{4}$$

Here, the control input is the spin speed Ω_i of each rotor that produces thrust $T_i = k_T\,\Omega_i^2$ azimuthal moment $\tau_i = k_M\,\Omega_i^2$. Furthermore, u_i is the rotor's spin axis expressed in body frame, r_i is the body-frame position vector from the vehicle's center of mass (CoM) to rotor i and $\widehat{\omega}$ is the skew-symmetric matrix satisfying $\widehat{\omega}x = \omega \times x$. Finally, $F_{\text{drag}} = -\,c_d\,m\,v$ is a linear aerodynamic drag opposing the body's velocity, and F_{downwash} represents the aerodynamic downwash force induced by nearby quadcopters [14]. We neglect the inertia of the rotors and instead assume that we can directly control their rotational speed.

IV. METHOD

We formulate the pursuit–evasion task as a continuous-control problem and train neural network policies for both the pursuer and evader via deep reinforcement learning (DRL) in a high fidelity simulator, see Section V. Our policies directly command body-frame angular rates and collective thrust, enabling aggressive, high-speed maneuvers. Training is performed in NVIDIA Isaac Sim, which integrates full rigid-body quadrotor dynamics at 62,5 Hz [15]. Episodes take place in a bounded 3D arena with randomized initial positions for pursuer and evader; each episode terminates upon capture (inter-drone distance below a threshold) or when a maximum time is reached. The DRL algorithm of choice is Proximal Policy Optimization (PPO) [16], which we use to optimize stochastic policies π_θ.

A. Policy Learning in Simulation

Each agent's policy π_θ is a three-layers Multi-Layer Perceptron (MLP) that maps observations o_t to actions

$$a_t = \left[\omega_x,\ \omega_y,\ \omega_z,\ T/m\right],$$

where $\omega_x, \omega_y, \omega_z$ are desired body-frame rates and T/m is the mass-normalized collective thrust. We bound each ω within $\pm\omega_{\max}$ and T/m within $[0,\ T_{\max}/m]$ to respect the quadrotor's actuator limits. These body rates and thrust are then tracked by a PID controller which outputs rotor commands Ω_i.

At time t, the observation o_t consists of:

- The current time t.

- The current and 4 past relative positions of the opponent $[\Delta p_{t-4:t}]$, where $\Delta p = p_{\text{opponent}} - p_{\text{self}}$. We have no assumptions about the opponent's nature or dynamics, we only observe their positions.
- Either the current global position p_t for the evader or the agent's altitude z_t for the pursuer.
- The agent's own rotation matrix $R_{\text{self}} \in SO(3)$, linear velocity $v_{\text{self}} \in \mathbb{R}^3$ and body rates $\omega_{\text{self}} \in \mathbb{R}^3$.

Define $d_t = \|\Delta p_t\|$, $\delta_t = 1_{\{d_t < \varepsilon\}}$, and $\tau_t = 1_{\{t = T_{\max}\}}$. Let κ_{a} weight approach/escape distance, κ_{br} weight body-rate magnitude, κ_{c} weight capture, κ_{t} weight timeout escape/penalty, and κ_{b} weight out-of-bounds. We define the following rewards:

- *Approach:* $r_{\text{approach},t} = \kappa_{\text{a}}\,(d_{t-1} - d_t)$.
- *Body-rate regularization:* $r_{\omega,t} = \kappa_{\text{br}}\,\|\omega_t\|$.
- *Capture event:* $r_{\text{catch},t} = \delta_t\,\kappa_{\text{c}}$
- *Out-of-bounds penalty:*

$$r_{\text{bounds},t} = \kappa_{\text{b}} \times \begin{cases} 1_{\{z_t < z_{\min}\}}, & \text{(pursuer)}, \\ 1_{\{p_t \notin \mathscr{A}\}}, & \text{(evader)}. \end{cases}$$

- *Timeout reward/penalty:*

$$r_{\text{timeout},t} = \begin{cases} \kappa_{\text{c}}, & \text{if } \tau_t = 1, \\ 0, & \text{otherwise}. \end{cases}$$

- *Step win:* $r_{\text{step}} > 0$.

Then the per-timestep rewards are:

$$r_t^{\text{p}} = r_{\text{approach},t} - r_{\omega,t} + r_{\text{catch},t} - r_{\text{bounds},t} - r_{\text{timeout},t}, \quad (5)$$

$$r_t^{\text{e}} = r_{\text{step}} - r_{\omega,t} - r_{\text{catch},t} - r_{\text{bounds},t} + r_{\text{timeout},t}. \quad (6)$$

Summing up Equation (5) and Equation (6) does not yield 0, thus the problem is not formulated as a Zero-Sum Game. The motivation is that $r_{\text{approach},t}$ serves as a good dense-reward for the pursuer. On the other hand, the evader should not be incentivized for maximizing its distance to the pursuer, but rather to maximize survival time.

B. Asynchronous Multi-Stage Population-Based Training

To mitigate nonstationarity and catastrophic forgetting when co-training two adversarial policies, we propose the *Asynchronous Multi-Stage Population-Based* (AMSPB) scheme. Figure 2 illustrates the overall pipeline. Starting from a small seed population of heuristics-based policies for both pursuer and evader, we repeat:

1) **Select Stage.** Alternate which side trains next. If the previous stage trained the pursuer, the next stage trains the evader, and vice versa.
2) **Sample Opponent.** With probability p_{old}, sample an "older" policy from the opponent's population; otherwise, sample the most recent policy. This ensures continual exposure to previously encountered strategies.
3) **Train Policy.** Using PPO, train a *new* policy for the selected side against the fixed sampled opponent for a fixed number of timesteps.

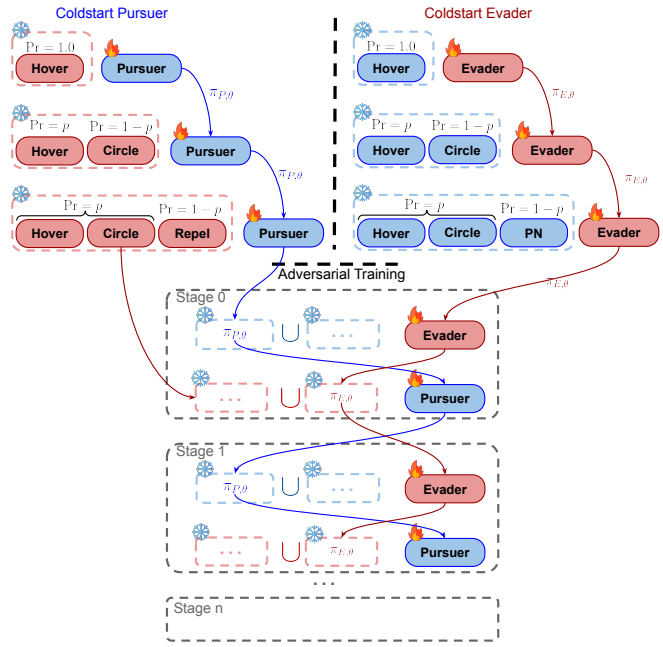

Fig. 2. Overview of the AMSPB training loop. After an initial "cold start" against heuristic controllers, each stage alternates training between pursuer and evader. At each stage, the newly introduced policy is trained against a sampled opponent (possibly from the pool of older policies). Successful policies enter the population, guaranteeing monotonic improvement and retention of earlier strategies.

4) **Evaluate and Update Population.** Once training completes, we add the learned policy into the pool of adversaries.

This setup ensures that each new policy must both outperform current adversaries and maintain competence against earlier strategies, resulting in robust, adaptive behaviors under adversarial conditions.

V. EXPERIMENTS

A. Simulation Environment

All experiments are conducted in NVIDIA Isaac Sim, where we simulate the AscTec Hummingbird quadrotor model with nominal parameters collected in Table I. We run 256 parallel environments for faster data collection. Each episode takes place in a bounded 10 m × 10 m × 4 m arena with randomly sampled initial poses for pursuer and evader. An episode terminates when the inter-drone separation falls below 0.5 m or when a maximum of 600 time steps ($\sim 8s$) is reached. All continuous observations are scaled to lie approximately in $[-1, 1]$. The parameters used to scale them are shown in Table II while Table III collects the hyperparameters of PPO.

Table IV lists the per-term coefficients used in the pursuer's and evader's reward functions.

B. Monotonic Improvement with Past Policies

To evaluate the effect of sampling past opponent policies during training, we compare our method (AMSPB) with [9] (AMS-DRL). Table V and Table VI report, for each variant,

TABLE I

NOMINAL HUMMINGBIRD QUADROTOR PARAMETERS.

Parameter	Nominal Value
Mass m [kg]	0.716
Inertia $[I_{xx} = I_{yy}, I_{zz}]$ [kg·m²]	[0.007, 0.007, 0.012]
Arm length l [m]	0.17
Drag coefficient c_d	0.2
Rotor force constant k_f [N·s²]	8.54858×10^{-6}
Rotor moment constant k_m [N·m·s²]	1.3677729×10^{-7}
Max rotor speed $\Omega_{\max}$ [rad/s]	838
Rotor configuration (angles) [rad]	$\{0, \frac{\pi}{2}, \pi, -\frac{\pi}{2}\}$

TABLE II

OBSERVATION NORMALIZATION FACTORS

Observation	Normalization Divisor
Time t	$T_{\max} = 600$
Relative position Δp	[10.0, 10.0, 4.0] m
Position p	[5.0, 5.0, 2.0] m
Altitude z	2.0 m
Linear velocity v	[15, 15, 5] m/s
Angular velocity ω	[15, 15, 5] rad/s

TABLE III

PPO HYPERPARAMETERS

Hyperparameter	Value
Learning rate	5×10^{-4}
Clip ratio	0.1
Discount factor γ	0.99
GAE λ	0.95
Batch size (per update)	2048
Epochs per update	4
Entropy coefficient α_{ent}	0.001
Value loss coefficient	1.0
Max gradient norm	5.0

TABLE IV

REWARD COEFFICIENTS

Coefficient	Value
Distance weight κ_a	0.05
Body-rate penalty κ_{br}	0.0005
Capture bonus/penalty κ_c	10.0
Timeout (escape) κ_t	10.0
Out-of-bounds penalty κ_b	0.1
Step penalty r_{step}	0.005

TABLE V

EVADER-CAUGHT RATES UNDER AMSPB (SAMPLING PROBABILITY 0.75). "—" INDICATES THAT THE CORRESPONDING OPPONENT HAD NOT YET BEEN INTRODUCED AT THAT STAGE. NOTE HOW PERFORMANCE AGAINST EARLY OPPONENTS, LIKE HOVER AND CIRCULAR, ARE KEPT HIGH FOR ALL STAGES.

Stage	**Hover**	**Circular**	**Repel**	**Rate:s0**	**Rate:s1**	**Rate:s2**
1	0.9805	—	—	—	—	—
2	0.9531	0.9727	—	—	—	—
3	0.9961	1.0000	0.8906	—	—	—
4	0.9297	0.9609	0.6797	0.4062	—	—
5	0.9570	0.9883	0.8516	0.6836	0.6055	—
6	0.9766	0.9961	0.8086	0.6289	0.5703	0.4297

TABLE VI

EVADER-CAUGHT RATES UNDER AMS (SAMPLING PROBABILITY 0.0)."—" INDICATES THAT THE CORRESPONDING OPPONENT HAD NOT YET BEEN INTRODUCED AT THAT STAGE. NOTE HOW PERFORMANCE AGAINST EARLY OPPONENTS, LIKE HOVER AND CIRCULAR, ARE DETERIORATING FOR THE LATER STAGES.

Stage	**Hover**	**Circular**	**Repel**	**Rate:s0**	**Rate:s1**	**Rate:s2**
1	0.9805	—	—	—	—	—
2	0.9570	0.9883	—	—	—	—
3	0.9922	0.9961	0.9180	—	—	—
4	0.8906	0.6406	0.8672	0.7383	—	—
5	0.8906	0.6797	0.6055	0.2305	0.4570	—
6	0.6445	0.8086	0.4727	0.6875	0.1602	0.1758

the fraction of episodes in which the pursuer successfully catches the evader ("Evader_caught") when evaluated against a fixed suite of benchmark strategies. The columns correspond to progressively harder opponents introduced over training. Each row shows results after a new policy enters the population. For example, "Rate:s0" is the first rate-based policy added, "Rate:s1" the second, and so on.

From Table V, we observe that when sampling past policies, the newly trained policy consistently maintains high capture rates against all previously introduced opponents (*Hover*, *Circular*, and *Repel*). Even after introducing successive rate-based strategies (*Rate:s0*, *Rate:s1*, *Rate:s2*), performance against earlier benchmarks remains strong, demonstrating stable, monotonic improvement. In contrast, Table VI shows that when older policies are never sampled, the capture rate against early opponents degrades over time. For example, after the sixth stage (*Rate:s2*), the policy's success against *Hover* drops to 0.6445 and against *Repel* to 0.4727. The precipitous decline in "Evader_caught" rates highlights overfitting to the latest adversary and forgetting of previously learned strategies.

C. Velocity- vs. Rate-Based Controllers

To evaluate generalization to unseen opponent styles, we perform cross-policy matchups in which a pursuer trained with one command modality faces an evader trained with the other. Table VII reports the fraction of episodes in which the evader is caught ("Evader_caught") for each combination of pursuer and evader policies. When the pursuer uses a rate-based policy against a velocity-based evader, the evader is caught in 57.03% of trials. Conversely, if the pursuer is velocity-based and the evader uses a rate-based policy, the evader is caught only 13.67% of the time. This demonstrates that rate-based controllers can better exploit the quadrotor's full dynamics and perform better in a scenario not seen during training.

In addition, we measure the maximum free-flight linear and angular velocities achievable by each policy. Table VIII lists these peak speeds. The rate-based policy attains a top linear speed of 12.90 m/s and an angular rate of 12.85 rad/s,

TABLE VII

EVADER CAPTURE RATES IN CROSS-MODALITY MATCHUPS UNSEEN DURING TRAINING.

Pursuer	Evader	Evader_caught
Rate	Velocity	0.5703
Velocity	Rate	0.1367

whereas the velocity-based policy peaks at 10.49 m/s and 6.38 rad/s, respectively. These results confirm that body-rate commands enable the agent to better exploit the quadrotor's actuation limits and achieve more agile maneuvers.

TABLE VIII

MAXIMUM ACHIEVABLE LINEAR AND ANGULAR VELOCITIES.

Policy	Max linear vel (m/s)	Max angular vel (rad/s)
Rate	12.90	12.85
Velocity	10.49	6.38

VI. CONCLUSIONS

We have introduced a simulation-based RL framework for 1v1 quadrotor pursuit–evasion, leveraging body-rate control, and a continual adversarial-population-based training loop (AMSPB). Our policies learn to exploit the full nonlinear dynamics for both pursuer and evader roles. The AMSPB algorithm alternates learning between sides while sampling from a growing population of past opponents, ensuring monotonic performance gains and preventing catastrophic forgetting. Empirically, rate-based controllers outperform velocity-level baselines in capture rates and peak speeds, and AMSPB agents maintain high success against increasingly difficult strategies.

REFERENCES

[1] S. Park, H. T. Kim, S. Lee, H. Joo, and H. Kim, "Survey on Anti-Drone Systems: Components, Designs, and Challenges," *IEEE Access*, vol. 9, pp. 42 635–42 659, 2021.

[2] W. Du, T. Guo, J. Chen, B. Li, G. Zhu, and X. Cao, "Cooperative pursuit of unauthorized UAVs in urban airspace via Multi-agent reinforcement learning," *Transportation Research Part C: Emerging Technologies*, vol. 128, p. 103122, Jul. 2021.

[3] M. Pliska, M. Vrba, T. Báča, and M. Saska, "Towards Safe Mid-Air Drone Interception: Strategies for Tracking & Capture," *IEEE Robotics and Automation Letters*, vol. 9, no. 10, pp. 8810–8817, Oct. 2024.

[4] E. Kaufmann, L. Bauersfeld, and D. Scaramuzza, "A Benchmark Comparison of Learned Control Policies for Agile Quadrotor Flight," Feb. 2022.

[5] D. Hanover, A. Loquercio, L. Bauersfeld, A. Romero, R. Penicka, Y. Song, G. Cioffi, E. Kaufmann, and D. Scaramuzza, "Autonomous Drone Racing: A Survey," *IEEE Transactions on Robotics*, vol. 40, pp. 3044–3067, 2024.

[6] Y. Song, A. Romero, M. Müller, V. Koltun, and D. Scaramuzza, "Reaching the limit in autonomous racing: Optimal control versus reinforcement learning," *Science Robotics*, vol. 8, no. 82, p. eadg1462, Sep. 2023.

[7] C. de Souza, R. Newbury, A. Cosgun, P. Castillo, B. Vidolov, and D. Kulić, "Decentralized Multi-Agent Pursuit Using Deep Reinforcement Learning," *IEEE Robotics and Automation Letters*, vol. 6, no. 3, pp. 4552–4559, Jul. 2021.

[8] R. Zhang, Q. Zong, X. Zhang, L. Dou, and B. Tian, "Game of Drones: Multi-UAV Pursuit-Evasion Game With Online Motion Planning by Deep Reinforcement Learning," *IEEE Transactions on Neural Networks and Learning Systems*, vol. 34, no. 10, pp. 7900–7909, Oct. 2023.

[9] J. Xiao and M. Feroskhan, "Learning Multipursuit Evasion for Safe Targeted Navigation of Drones," *IEEE Transactions on Artificial Intelligence*, vol. 5, no. 12, pp. 6210–6224, Dec. 2024.

[10] A. Ghotavadekar, F. Nekovář, M. Saska, and J. Faigl, "Variable Time-Step MPC for Agile Multi-Rotor UAV Interception of Dynamic Targets," *IEEE Robotics and Automation Letters*, vol. 10, no. 2, pp. 1249–1256, Feb. 2025.

[11] M. Kouzeghar, Y. Song, M. Meghjani, and R. Bouffanais, "Multi-Target Pursuit by a Decentralized Heterogeneous UAV Swarm using Deep Multi-Agent Reinforcement Learning," in *2023 IEEE International Conference on Robotics and Automation (ICRA)*, May 2023, pp. 3289–3295.

[12] E. Çetin, C. Barrado, and E. Pastor, "Countering a Drone in a 3D Space: Analyzing Deep Reinforcement Learning Methods," *Sensors*, vol. 22, no. 22, p. 8863, Jan. 2022.

[13] M. Faessler, A. Franchi, and D. Scaramuzza, "Differential Flatness of Quadrotor Dynamics Subject to Rotor Drag for Accurate Tracking of High-Speed Trajectories," *IEEE Robotics and Automation Letters*, vol. 3, no. 2, pp. 620–626, Apr. 2018.

[14] K. P. Jain, T. Fortmuller, J. Byun, S. A. Mäkiharju, and M. W. Mueller, "Modeling of aerodynamic disturbances for proximity flight of multirotors," in *2019 International Conference on Unmanned Aircraft Systems (ICUAS)*, Jun. 2019, pp. 1261–1269.

[15] B. Xu, F. Gao, C. Yu, R. Zhang, Y. Wu, and Y. Wang, "OmniDrones: An Efficient and Flexible Platform for Reinforcement Learning in Drone Control," Sep. 2023.

[16] J. Schulman, F. Wolski, P. Dhariwal, A. Radford, and O. Klimov, "Proximal Policy Optimization Algorithms," Aug. 2017.